

EVALUATION OF ASWING FOR OVERALL AIRCRAFT DESIGN OF UNCONVENTIONAL CONFIGURATIONS. APPLICATION TO JOINED WINGS WITH FOLDING WINGTIPS

Romain JAN1, Scott DELBECQ1 & Emmanuel BENARD1

¹Fédération ENAC ISAE-SUPAERO ONERA, Université de Toulouse, France

Abstract

This paper presents an experimental evaluation of an aeroelastic framework (ASWING) for the longitudinal aerodynamic characteristic, structural response and buckling of joined wings. It also studies the effect of folding wingtips on this type of layout. Aswing is shown to be a suitable multidisciplinary tool for the design of unconventional layout. An application example is proposed with a joined wing having folding wingtips. The latter are shown to bring a wing structural mass saving of up to 15%. The association of joined wing with FFWT brings a 48% mass saving. From a Breguet analysis the joined wing could bring between 6.5 to 12.5 % fuel savings compared to conventional layouts for the same design mission. If the Paylaod is extended, the gain in PFEI varies from 17,2 to 33,3%. Thanks to bigger tanks, this layout can carry the same design between 31,5 and 32,3% further. The airplanes ultimate range is increased between 32,43% and 63,7%. The gain increases with the payload range product of the aircraft. For larger airplanes, the wing and horizontal stabilizer masses account for a greater proportion of the structure aircraft mass, increasing the benefit brought by the joined wing and Flared Folding Wing tips; explaining the above large performances improvements intervals

Keywords: Aircraft Design, Conceptual Design, Joined Wings, Flared Folding Wing Tips

1. Introduction

The growing interest in environmental sustainability pushes the aviation research community and industry to investigate all the potential levers. The main four levers are 1 - demand/supply management, 2 - operations efficiency, 3 - aircraft efficiency and 4 - decarbonization of energy carriers [1]. This paper focuses on the aircraft efficiency lever. Incremental improvements are anticipated in the short term, resulting in gradual aircraft efficiency gains, while disruptive innovations have the potential to achieve substantial gains in the medium to long term [1]. Among the disruptive technologies, unconventional aircraft configurations are expected to offer the most significant benefits, primarily through the development of highly optimized airframes, with or without the integration of advanced propulsion systems [2].

Among them, one can find the Aurora D family, a concept developed by Aurora in collaboration with the Massachusetts Institute of Technology (MIT), represents a significant leap forward in addressing these goals. Known for its distinctive "double-bubble" fuselage and the implementation of boundary layer ingestion (BLI) technology, the D6, 8 and 12 promise substantial reductions in fuel consumption, emissions, and noise levels compared to conventional airliners [3]. Other examples of unconventional configurations are those that involve high aspect ratio wings to improve aerodynamic efficiency such as the strut-braced wing or twin-fuselage configurations [4]. To improve aerodynamic efficiency other concepts such as the flying-V [5] and box-wing [6] are also evaluated

This paper proposes to further push the boundaries of aerodynamic and structural efficiency, by evaluating ASWING [7] in the overall aircraft design of unconventional configurations. Such an evaluation is mandatory before exploring integration possibilities of ASWING in overall aircraft design frameworks. To this end, the unconventional configuration application chosen is the joined wing

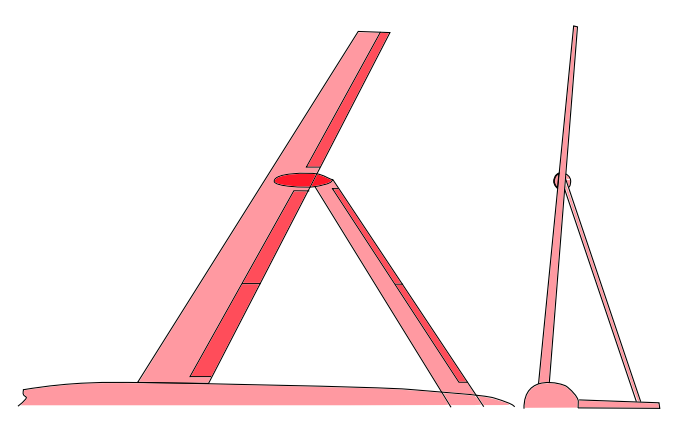


Figure 1 – Illustration of the Joined Wing Concept

(also sometimes referred to as box-wing). This concept (cf figure 1), characterized by its closed-loop structure connecting the main and tail wings, offers potential advantages in reducing aerodynamic drag and improving load distribution across the airframe in comparison to conventional wings (tapered swept wings and horizontal stabilizer). Wolkovitch [8] showed particularly that at Iso-structural weight, a diamond joined wing can show significant drag saving. While Kroo et al [9] have shown that at Iso-aerodynamic performance, a joined wing could provide a structural mass saving of 40%. Predictions are also verified experimentally by Lin et al' work [10]. Both advantages are incompatible in terms of joint location but a tradeoff can be found. Moreover Joined wings also delays the flutter onset in comparison to conventional wing as reported by Stearman [11] and provide a significant structural relief to the fuselage during emergency landing. Finally joined wing aircraft can provide direct lift and side force control [8]. In consequence, joined wing might be a serious candidate for future aircraft design.

No matter the wing platform considered (strut-braced, cantilever, joined wing etc), another system of interest can drastically help reducing the structure mass and enhance the aircraft maneuverability. The latter is known as Folding Wingtip or Flared Folding Wing Tip (FFWT). Initially created to reduce the wing span in order to avoid paying extra gateway taxes, folding wingtips can show real advantages in flight. In particular, they can provide important load alleviation during gust encounter. Bristol university has particularly studied this type of devices through the successive work of Castrichini [12, 13], Cheung [14, 15], and Healy [16, 17]. They all have successively showed that Folding Wing Tip devices provide important root bending moment relief during gust encounter. Healy has also proved that Folding Wing Tip when they are released during a roll maneuver, they improve the rolling rate of wings [18]. This is of particular interest as those aforementioned aircraft platforms tend to have higher aspect wings, so higher rolling inertia and aerodynamic damping leading to poor lateral performance in maneuver. Finally, Healy showed that folding wing tip equilibrium is very sensitive to cross-wind condition [17], where they could be used (landing with strong cross wind). In consequence, Flared Folding Wing Tip represent a real lever, to improve the structural performances of any of the platform mentioned above. However, their behaviour is quite sensitive to the flight condition and must be accurately captured.

In light of the previous comments, this paper proposes a methodology of evaluation of what could be the mass saved in comparison to a classical layout, if a joined wing is coupled with Flared Folding Wing Tips.

Integrating ASWING into overall aircraft design framework such as FAST-OAD [19] would enable comprehensive aeroelastic analysis and simultaneous optimization of aerodynamic, structural, and potentially control system parameters, leading to more efficiency aircraft designs. The benefits of integrating external tools for more accurate discipline analysis has already been outlined with other tools [20]. While wrapping external tools is relatively simple in Python or through Functional Mock-up Units, it may lead to increased computation time, which could hinder the decision-making processes in conceptual or preliminary design stages [21]. These integration aspects will be evaluated also in this paper.

For this purpose, the paper is organized as follows. Section 2 presents the analysis framework

used in this paper. Section 3, 4 and 5 present its experimental validation to make sure it captures well, the longitudinal characteristic, structural response and buckling of joined wings configuration. In section 6, Aswing is evaluated against Healy's experimental data related to the lateral and longitudinal behaviour of Flared Folding Wing Tips. Then in light of the comparison with the experiments, an application example is proposed in section 7 to assess the benefit of coupling Flared Folding Wing Tips with joined wing platform on 6 different scenarios using a Breguet analysis.

2. Aeroelasticity framework: Aswing

Many aeroelasticity frameworks exist, but Aswing from MIT [7] has been shown to be the one that offers the many features and to be very efficient [22]. In this paper, it is used to provide some lowfidelity aeroelastic analysis of the layouts of interest. Aswing uses an extended Euler-Bernoulli beam theory coupled with an unsteady nonlinear lifting-line or slender-body theory to model flexible wings and fuselages [23, 24]. Various layouts can be modeled, such as cantilever, strut-braced, joined, boxed, and tandem wings. Distributed propulsion can also be considered as well as folding wingtip devices. As a result, it is a good candidate for the pre-design analysis of the next generation of aircraft. Thanks to its FORTRAN implementation, Aswing is very efficient and can be considered for heavy multi-variables aircraft design optimization problems. This software has been evaluated on several experimental cases presented in 4 technical reports published by Jan with separate focus on 1 - aerodynamics [25], 2 - propellers [26], 2 - structure [27] and 4 - aeroelasticity [28]. This series of reports shows that Aswing can be used as a pre-design framework for the various configurations mentioned above. In the next 4 sections, an experimental validation of Aswing on the prediction of the aerodynamics and structural response of the joined wing and folding wingtips is presented to reinforce this paper's methodology and also highlight its limitations. For the sake of transparancy, every experimental data and Aswing simulations are available in a Git-Hub repository. The reader will find all the simulations data, experimental data extracted from the literature (please refer to original cited works). The reader must have an Aswing and Matlab licence to fully take benefit of this data. The repository can be found following this hyper-ref link: ICAS-2024-Jan-Git

3. Aerodynamics of joined wing: longitudinal characteristic and control

Before considering any design analysis, it is important to make sure that the framework used for the latters, provides reasonably good agreements with experiments or higher fidelity data, specially in relation to the layouts of interest that is the joint wing here. In the case of pre-design analysis, capturing correctly the longitudinal characteristic of an aeroplane is mandatory, as it plays an important role on the sizing of each element in order to have a well balanced and stable/controllable aircraft. Thus a focus is made on this aspect in this section.

A very specific type of interaction can occur on Diamond or joined wings such as the one depicted in figure 2-(a). When two lifting surfaces cross sections are near enough, the rear wing can influence the flow curvature of the forward wing because of its own circulation as illustrated in figure 2-(b). This in consequence modifies the local lift of the forward wing and can drastically distort it. On a conventional aircraft, the main wing geometry is initially optimised, its wake is computed and prescribe as an upstream condition of the horizontal stabilizer so that it can be designed. Its effect on the forward wing is neglected as it is far downstream. On joined wings aircraft, both the forward and rear wing must be optimized in the same time as reported and verified experimentally by Wolkovitch ([29, 8]. He showed that the complete flow field induced by every lifting surface of a joined wing must be solved simultaneously to provide good agreement with experiments where the Prandtl Bi-plane theory is showing weakness in this case. Wolkovitch also showed that its numerical simultaneous optimisation of the joined wing forward and rear geometry was showing real benefit.

Aswing is able to model and solve the flow field induced by numerous lifting surfaces. In contrast with Wolkovitch's numerical model ([29]) that was a vortex lattice panel method (VLM), Aswing uses a lifting line model (that is a very coarse VLM). Thus the comparison with experiments provided by Wolkovitch in [29] and [8] can not be invoked to assess the Aswing precision on this type of geometries. Thus in this section an evaluation adapted to Aswing is proposed To do so, the experimental data of Smith et al [30] have been used. In their work, they studied experimentally the longitudinal/lateral characteristic and controllability of a joined wings aircraft prototype. Three versions of the

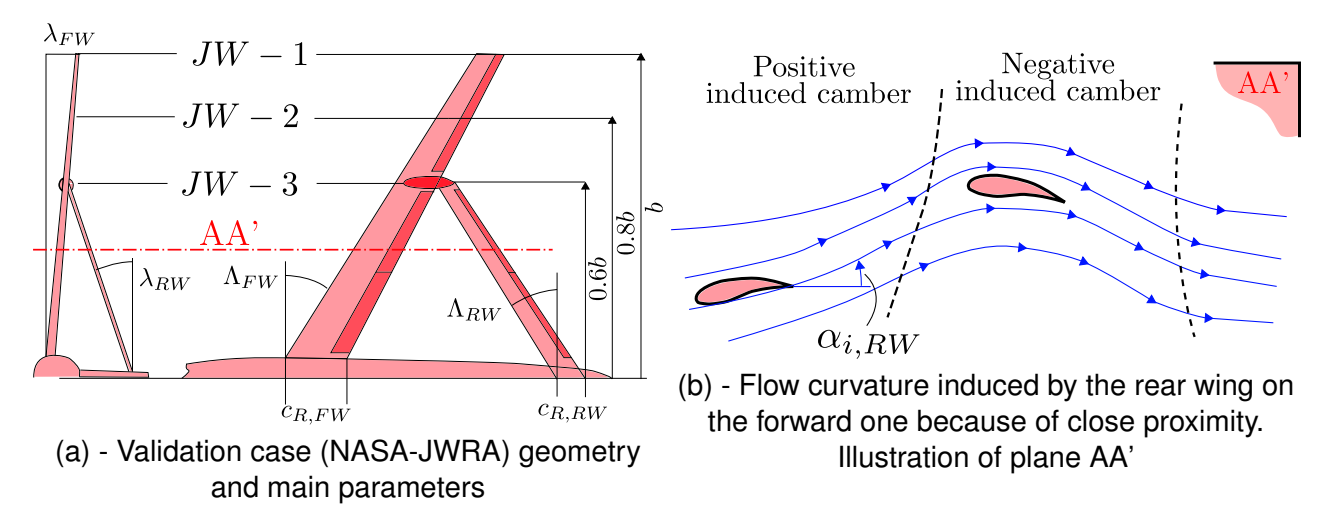


Figure 2 – Validation case (NASA-JWRA) : Diamond joined wing geometry and proximity effects

NASA joined wing prototype denoted as JWRA have been studied and are refereed as JW-1 to 3. Their geometries are illustrated in figure 2 (a) where the only difference in the version is the forward wing span length with JW-3 having the shortest. A complete detail of the geometric parameters and airfoils of each version can be found in table I and II of Smith's technical report [30].

The experiments took place in a 12 foot pressure wind tunnel at a fixed dynamic pressure of $170lb/ft^2$ for longitudinal measurements and $90lb/ft^2$ for lateral measurement because of rolling moment constraint on the measurements balance. The equivalent Reynolds number were 1E6 and 0.625E6. The transition of the boundary layer of each lifting surfaces boundary layer were tripped at 0.35c. Overall, many tests have been performed and we have digitized the data. In this article, only the longitudinal characteristic and pitch control of the JW1 to 3 are presented, as too much geometric parameters are missing to model accurately the lateral behaviour of the JWRA prototypes.

Numerically, each bench have been reproduced and XFOIL analysis of each airfoil have been performed at the wind tunnel condition. Figures 2 (a) to (c) present the lift, drag and pitching moment comparison between the Aswing 5.98 predictions and Smith's measurements [30] for each JW prototype.

For the lift no matter the version, the Aswing predictions are in excellent agreement with the experiments on the linear range, with a slope error below 7% in the worst case. Aswing also captures the early stall of each configuration. Out of the linear range, Aswing is not able to capture the drop in lift and thus present a constant offset for the upper value of angle of attack for which the lift starts to rise again.

Secondly, Aswing captures well the drag of each configuration as long as a perfect knowledge of the wind tunnel condition is provided. The small rise in discrepancies at moderate angle of attack are due to the constant profile drag coefficient, that has been corrected in our modified version of the code. At post stall angle of attack, Aswing loses the track with the measurements.

For the pitching moment, Aswing captures well the linear moment slope $C_{M,\alpha}$ with the same level of error as for the linear lift slope $C_{L\alpha}$. Thus Aswing will provide good stability prediction. However, on the JW-1 and 2 prototypes, Aswing returns a constant offset with the measurements while for the third case, the predictions are in excellent agreement.

The constant off set can be explained by the fuselage lift carry over. Indeed, the latter carries a part of the wing lift because the wing flow-field tends to change the pressure distribution on the fuselage cross section. The theorem of the circle states that an antisymetric imaginary shrinked vortex sheet placed inside the fuselage to ensure an impermeability condition on its section can be used to model this interaction. If the positions of a vortex horseshoe corner positions are denoted as the complex \mathscr{Z}_1 and \mathscr{Z}_2 in the (z,y) plane, their image location in the fuselage are given as $\mathscr{Z}_{i,1} = R^2/\mathscr{Z}_1$ and $\mathscr{Z}_{i,1} = R^2/\mathscr{Z}_2$ where R is the fuselage radius. The Kutta-Joukowski theorem is then integrated on the image vortex sheet to get the lift carry over by the fuselage. From the definition of $\mathscr{Z}_{i,1}$, the latter

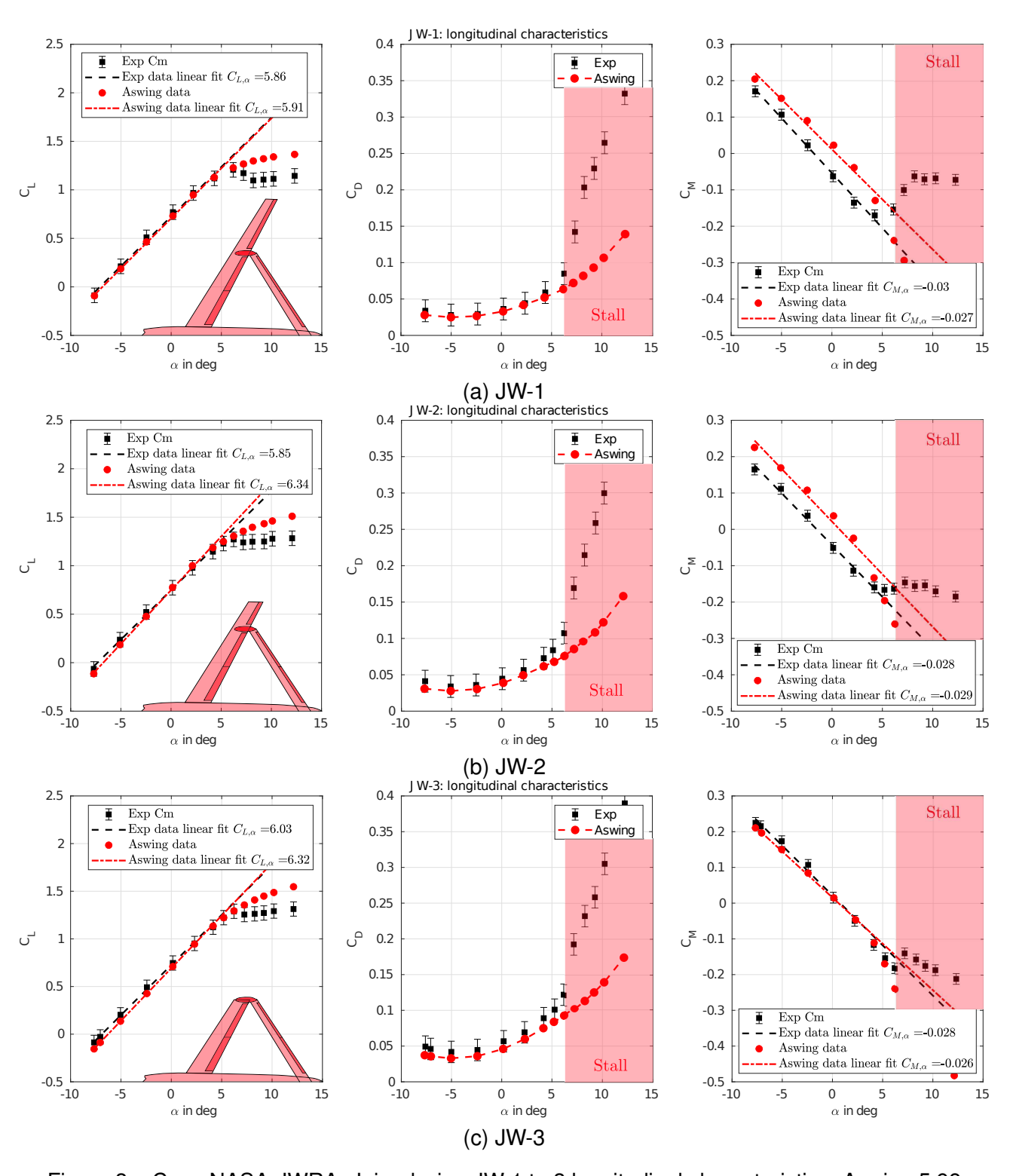


Figure 3 – Case NASA-JWRA: Joined wing JW-1 to 3 longitudinal characteristics. Aswing 5.98 prediction against experimental data from Smith [30]

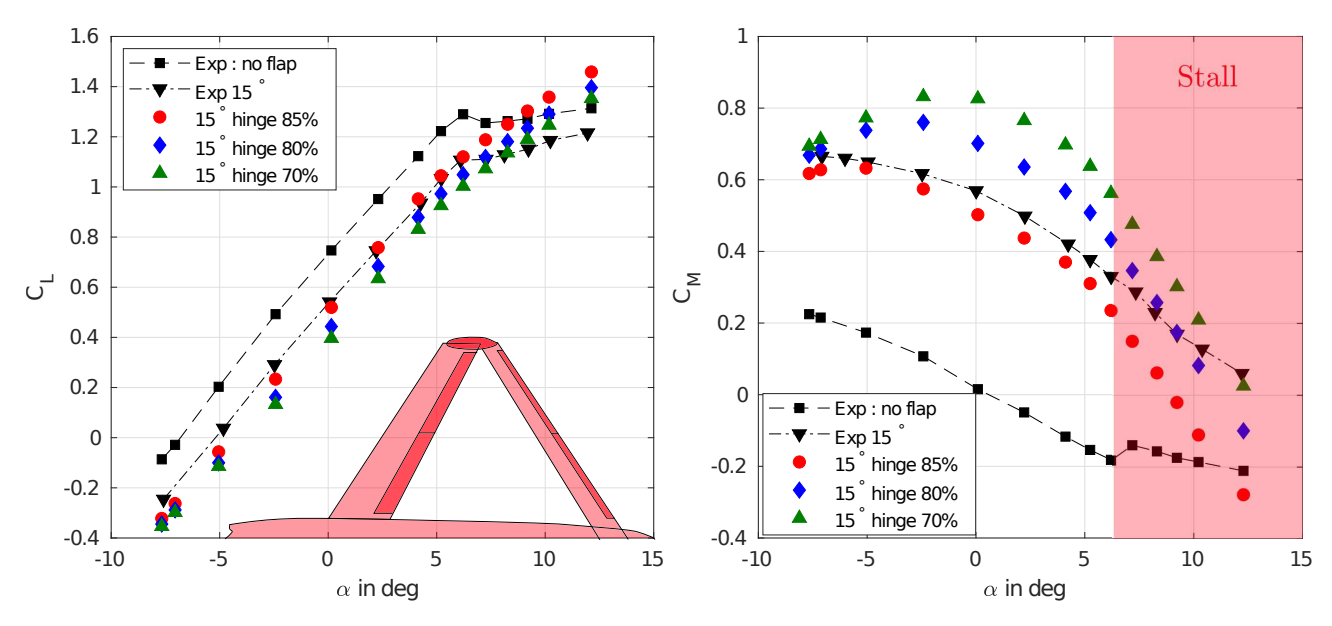


Figure 4 – Case NASA-JWRA: Joined wing JW-3 Longitudinal control. Rear wing inboard and outboard flap deflected at 15°. Aswing predictions for various hinge location against experimental data from Smith [30]

scales with $1/\mathscr{Z}_1$ so farthest is a vortex segment from the fuselage, smaller its image will be inside it. In the joined wing case JW-1 and JW-2, as the forward wing span is bigger, the lift carry over by the fuselage is lower than the one from the rear wing. This positive difference of lift between the rear and the front wing tend to induce a pitching down moment. As the fuselage lift carry over is a direct image of each lifting surfaces lift, the difference in lift is constant with the angle of attack, so the constant offset in the pitching moment observed. As Aswing is not modelling the fuselage lift carry over, it tends to overestimate the pitching moment of the JW-1 and 2 models. As for the JW-3 the wings spans are equal, no difference in lift is generated by the fuselage, so the good agreements with the experiments. This test case is thus very interesting to show how important can be the effect of the fuselage/wing interference on the longitudinal characteristics of joined wings aircraft. For example, in a pre-design analysis, such an offset in the pitching moment will tend to underestimate the rear wing elevator deflection to trim the aircraft at cruise condition and so underestimate the trim drag.

Smith [30] provided measurements of the longitudinal and lateral control derivatives. Unfortunately they did not give the hinge location of each flaps. Or the 2D flap derivatives are very sensitive to it. Thus several XFOIL analysis have been performed for various hinge location that are h/c = 0.7, 0.80, and 0.85. The latter are the most likely to fit the real one from a coarse analysis of the geometry images in the report. Also only the comparisons on the JW-3 case are presented as, it would accumulate to much error from the pitching moment offset observed on the JW1 and JW2 prototypes. Figures 4 left and right present the comparison between the Aswing predictions and the measurements of the effect of a deflected elevator on the lift and pitching moment. It seems that the flap derivatives for the hinge location of 85% provides the best agreements with the experiments for both lift and moment on the linear range. However the reader is invited to be careful about these conclusions as not all the necessary parameters were available for our analysis. From the latter, assuming that the lift carry over will be modeled in the future, Aswing should be able to trim correctly Joined wing aircraft with good trim drag predictions.

In conclusion, Aswing captures well the main effect which is dominant on joined wing aircraft that is the change of the forward wing flow curvature because of the rear wing circulation. Aswing can predict well, the lift and drag of such configurations, however, pitching moment tend to be over-predicted when the wings spans are different. This offset can be solved by modeling the fuselage lift carry over using the Theorem of the circle previously discussed in this section.

4. Static response of joined-wing for structural failure analysis

Among the features of Aswing, there is the joint connection. Beams can be connected through distant or close compliant/rigid joints. This feature is a of particular interest as it allows the structural study of joined wings. The main advantage of the latters is to provide considerable mass saving. Indeed, the structure, when its joint location is wisely chosen, take more advantage of the normal bending stiffness of the wing box. It allows the reduction of the wall thickness and thus a mass saving. Kroo et al [9] have showed for example that a 40% saving is possible in comparison to a cantilever swept wing with an horizontal stabilizer, leading to a significant fuel saving. Wing boxes walls are mostly designed to resist out of plane bending and vertical shear forces ([9]). Capturing the effect of a joint connection on those quantities, and their variation with the spanwize coordinate is of interest in aircraft design. In this case, the validation of Aswing is proposed using the experimental data of Lin et al[10]. In their work, they have studied the static response of the NASA-JWRA joined wing 1/6 scale prototype, with different load cases. This geometry is similar to the aerodynamic cases presented the previous section. Lin has studied up to 8 different joints allowing different degrees of freedom. In this work, only two of them are presented that are the rigid and "in-the-plane free translation" link joints. Those in particular, because they were the one presenting most important differences in performances and also the easiest one to extract the data from. The rigid joint is denoted as Case A while the "in-the-plane free translation" link joint is named Case B.

The geometry is a diamond wing, with the forward wing having a 5° dihedral angle and a 30° swept back angle. The wing is tapered with root and tip chord lengths respectively equal to 0.5638 and 0.2252 ft (0.1718 and 0.06864 meters). The wing span is 6.67 ft (2.03 meters) with an aspect ratio of 13. The JWRA prototype is composed also of a rear wing having a -20° dihedral angle and -32° swept forward angle. The wing is tapered with root and tip chord lengths respectively equal to 0.2476 and 0.1484 ft (0.07548 and 0.04523 meters). The wing span is 4 ft (1.21 meters) and is fixed to the forward wing at 60% of its span. The rear wing aspect ratio is 16. The 2 wings structural boxes parameters (mass, stiffness, inertia etc) are coarsely describe in Lin's work [10] (cf table 2.1 of his article), with only 3 spanwise discretization for the forward wing, and two for the rear wing. Discrepancies in Aswing prediction could come from the interpolation performed by the software. In total four load cases have been studied. Thirty pounds (13.5 kg) only on the forward wing, corresponding to a cantilever wing. The same load, but with forward wing carrying 90% of it and the rest for the rear. The two other load cases are 20 pounds (9.1 kg) with 90%-10% and 80%-20% load distribution. For every cases, the load distribution was following a cosine function in the spanwize coordinate as illustrated in figure 5-(a). The loads were produced using a system of pulleys at equally spaced spanwize location, with the tension fixed to recover the cosine function integrated on each segment. Finally the loads were applied on the elastic axis of each boxes (that is mid-chord). Out of plane bending moments on each wing were measured at different spanwize location, using differential strain gauges. The measurements were projected on the uptsream axis (x-axis in figure 5). Regarding the joints, the rigid one corresponds to a connection where all rotations and translations are matched between the forward and rear wing connection points. The "in-the-plane free translation" link joint consist of allowing x and y translations as-well as a z rotation. In consequence, only z translations, x and y rotations are matched. This can be performed through the use of two pivot joints connected between them with a in-the-plane linear rail mechanism as depicted in figure 6.

The numerical bench of this case has been built using the second linear mass and inertia distribution parameters of Aswing to reproduced the external cosine load. The mass was set negative to reproduce the aerodynamic load, artificially created by the pulley system. Aswing predictions for the **rigid joint** of the out of plane bending moment projected on x-axis $(M_x(y))$ are presented in figure 5 (b) to (d) for each load cases. As illustrated, no matter the cases, Aswing presents good agreement with the experiments, no matter the spanwise coordinate. It captures well the effect of the joint on the significant reduction of the root bending moment as illustrated in the figures. Same conclusions are done for the rear and the cantilever wing. The JWRA prototype was having a mass around 5kg, or the two load cases are greater corresponding to at least a 2.5G case. The predictions quality is constant

with the load case, so Aswing is suited for structural failure analysis and joined wing box design. Moreover according to figures 6 (a) to (c) Aswing also captures with the same level of agreement, the effect of compliant joints such as the **in-the-plane link joint** on the static response of a joined wing, and so no matter again the load cases. In those figures, the major drawbacks brought by this compliant joint can be highlighted. Because of the in-the-plane unmatched translation, the rear wing is no longer working as a strut in compression, and cannot relief the forward wing bending moment. Moreover, because of the free rotation on the z-axis, the forward and rear wing bending moments can not balance each other as effectively as for the rigid joint case. Thus the structure of the joint wing is as efficient as a cantilever layout, making the first one irrelevant. In consequence in the next part of this work, a rigid joint is considered as suggested from Lin's experimental observations [10]. As it has been shown in this and previous section, Aswing is able to predict well, both the aerodynamic longitudinal and structural characteristics, making it a good candidate for joined wing aircraft pre-design.

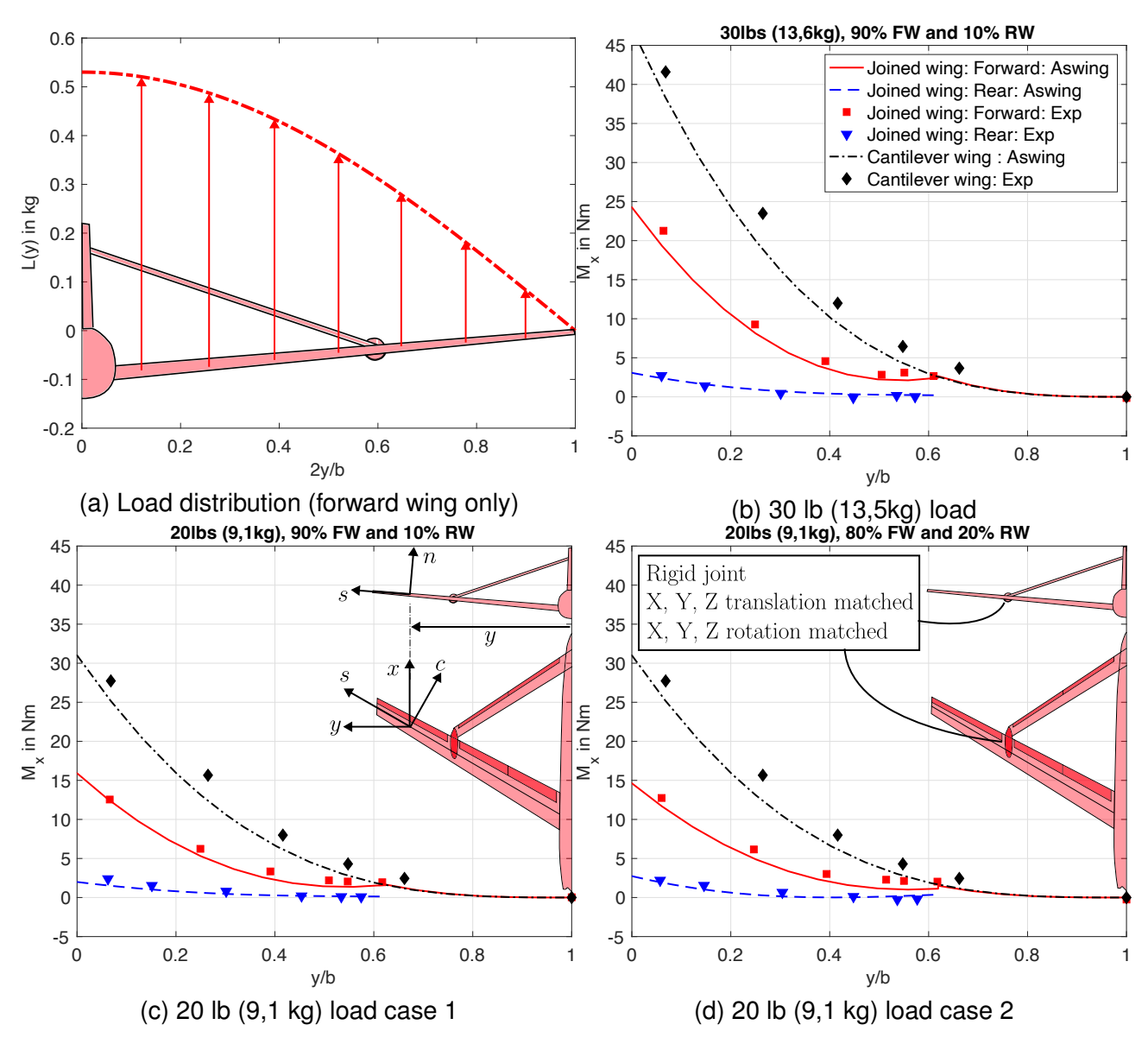


Figure 5 – Case NASA-JWRA: Joined wing, out of plane bending moment ASWING predictions against experiments of Stearman[11] and Lin[10]. Effect of a **rigid joint** against a cantilever wing. Effect of the load fraction carried by both wings. For figures (c) and (d) experimental data have been extrapolated from the 30 lbs load case for the cantilever wing.

5. Buckling of joined wing

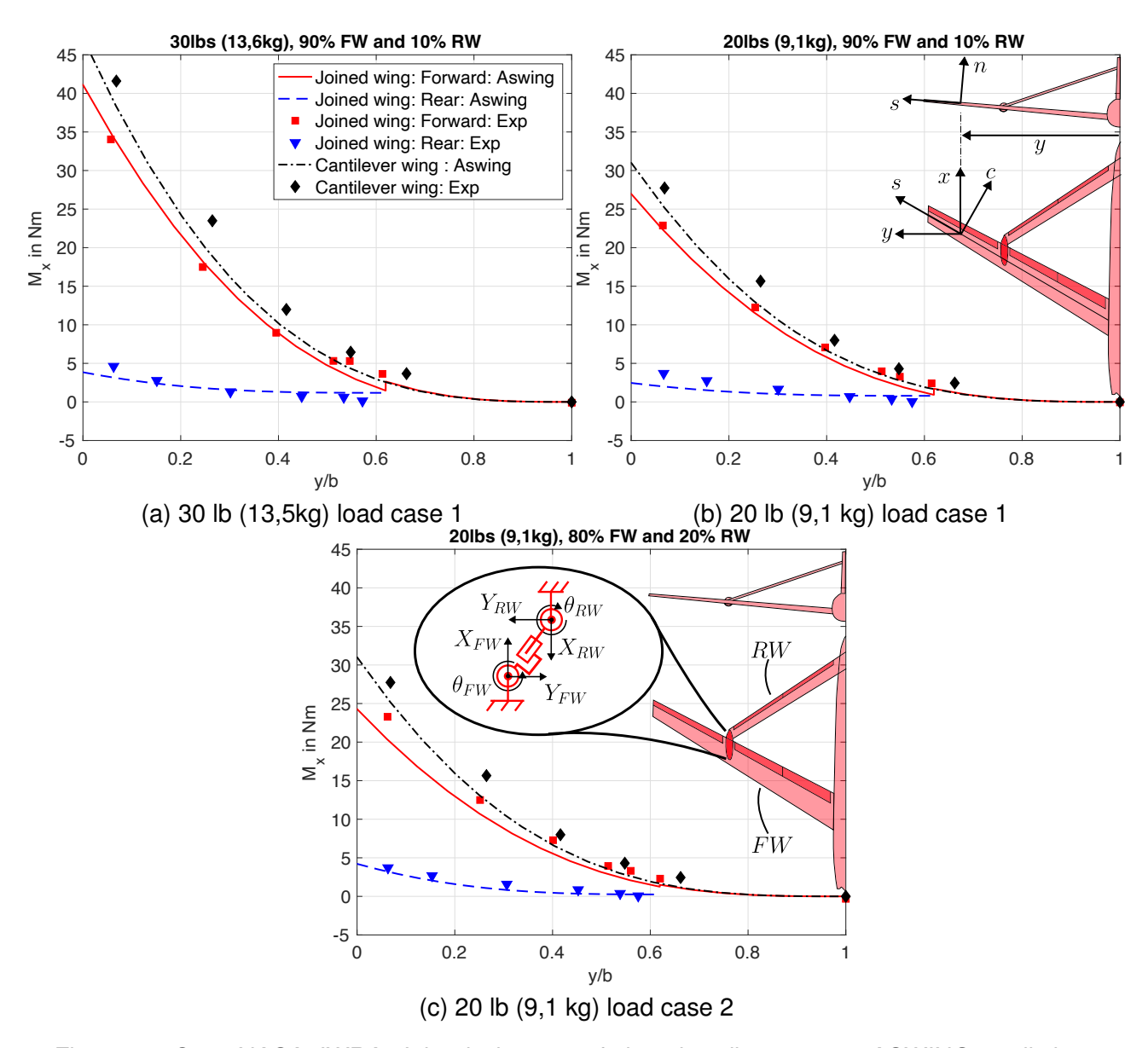


Figure 6 – Case NASA-JWRA: Joined wing, out of plane bending moment ASWING predictions against experiments of Stearman [11] and Lin[10]. Effect of a **link joint** against a cantilever wing. Effect of the load fraction carried by both wings. For figures (b) and (c) experimental data have been extrapolated from the 30 lbs load case for the cantilever wing.

5.1 Column buckling analysis of non uniform beams

New types of architectures such as strut-braced of diamond/joined wing rise new types of problems, because some of their structural components work in compression and can be subject to global buckling.

Original definition: The divergence due to buckling is defined by a critical axial load applied on a straight beam. This load defines the moment when; if an out of plane local displacement is applied (cf figure 7), the beam is no longer able to resist the bending moment induced by the axial load, using its structural bending stiffness properties. When the properties are non axis-symmetric, the divergence occurs in the plane of the weakest bending stiffness. The temporal response of the lateral displacement $\delta_x(t)$ is defined as a non harmonic divergence response. Thus from a modal analysis point of view, finding the critical load consists to find when a first pure real positive mode appears with the axial load rising. Euler provided analytical solutions of this problem for various cantilevering cases of beams. However, the major problem is that, this solution is only for uniform beams which is generally not the case for aeroplane structure. Aswing models such beams and thus extend the Euler solution to more complex structure.

5.2 Validation upon experimental data

As it was seen in the previous sub-section, Aswing is able to predict global buckling of any type of beams (uniform or not). Yet its precision for this phenomena is not known. This validation case, is particular, as it is not a direct validation. Indeed most of the column buckling test consist of placing a beam of a given length under a high load press. Each beam ends are pinned and are only free to rotate, or not. The problem in Aswing is that it is not possible to have a beam connected to 2 ground points to reproduce the above bench. Instead the upper end of the beam is free, and a tip mass can be applied to reproduce the axial load. The problem with this modeling technique is that it leads to discrepancies because of the different degrees of freedom of one of the ends. A modification of the code could be brought in order to solve it, but it will be pointless for aeroelasticity applications. It is important to note that the pinned-pinned cantilevering is possible as it has been seen in the joined wing case. The typical buckling test discussed earlier is just not possible to be reproduced.

Unfortunately, the latter is the one providing the widest and numerous range of experimental data. As Aswing's structural model is a non linear extension of the Euler Bernoulli beam theory, the predictions accuracy for buckling critical load calculations are recalled here. To do so, the experimental work of Niles et al[31] is used here. In their work, they have placed under a press, 5 different beams having various cross section (angle, zee, bar and rod). The latter are illustrated with their dimensions in figure 7. The beams are all made of aluminium alloy (14S-T), with an elastic modulus of 10,6E6 psi $(7.3E10Nm^{-2})$. For such cantilever configuration, the Euler analytical critical load is given by

$$F_{cr} = A \frac{\pi^2 E}{(KL/\rho)^2} \tag{1}$$

where E is the elastic modulus, K is the effective length factor set to 0.5 in this case, ρ is the minimum cross section radius of gyration, L is the length of the beam and, finally A is the cross section area. The quantity, KL/ρ is know to be the effective slenderness ratio, and is useful to detect the weakness of the Euler solution to predict the buckling load. The figure 7 (a) to (d) present a comparison, of the Euler critical load prediction with experimental measurements on the 5 beams. The latter have been denoted as Buckling cases A to E. The critical load is presented against the effective slenderness ratio, where the radius of gyration ρ is held fixed, and the length of the beam is varying. The Euler solution (and so by extension Aswing), gives good agreements with the experiments as long as the effective slenderness ratio is above 50, and so no matter the cases. The agreement of the Euler solution also confirms the hypothesis of considering only the minimum radius of gyration (ie minimal cross-section bending stiffness) for such analysis, as the cases B, C and D presenting important difference in the in-the-plane bending stiffness do not show significant prediction error changes. It is important to note, that Aswing does not neglect stiffer bending component in its modal analysis, in consequence, more complex buckling cases can be considered where lateral loads or bending moments can be involved such as it can happen on diamond/joined or strut braced wing. In consequence, the effective slenderness ratio can be used as an accuracy indicator for Aswing. As long

Evaluation of ASWING for overall aircraft design of unconventional configurations.

it is greater than 50, Aswing will provide good predictions of the critical buckling load of a structure. If the previous validation case is considered with the rear wing subject to compression, the slenderness ratio computed based on the bigger cross section (conservative) is equal to 58 which is above the recommended value. Aswing can be used in consequence to assess the buckling property of the JWRA prototype. If the slenderness ratio is below 50 there exist a modified version of the Euler solution called the Engesser equation. The reader can find a good explanation of it in Peery's book [32] (chapter 14, section 14.4 equation 14.16). This Engesser's solution is not really convenient for the Aswing beam formalism, as it is a direct solution. Instead, inspired from his work, a modification that could be brought to the code, would be to have a stall function for the Elastic Young modulus. Unfortunately, the latter is very dependant on the structure material. Such a model exists and is known as the Ramberg-Osgood equation, or the dimensionless form of tangent modulus curves (cf chapter 14, section 14.8, equation 11.19 of [32]), dropping the accuracy indicator value to 10. This, once implemented would provide Aswing the same level of accuracy as the one presented in Peery's work (cf chapter 14, section 14.4, figure 14.7).

Global not local buckling:

Aswing is able to predict the global buckling of a beam. The local skin buckling for example is not captured. From the bending and shear forces computed from the model, it is possible to detect it with a shear flow analysis code such as Co-Blade but it is not implemented natively in Aswing.

In conclusion, Aswing is able to predict the global divergent buckling of complex structure having a slenderness ratio above 50. It will be most likely the case, as modern aircraft, tends to high aspect ratio layouts increasing the accuracy indicator. As the critical load decreases rapidly with it, such aeroplanes are very likely to be subject to buckling. It is thus highly recommended to perform such analysis in conceptual design loops.

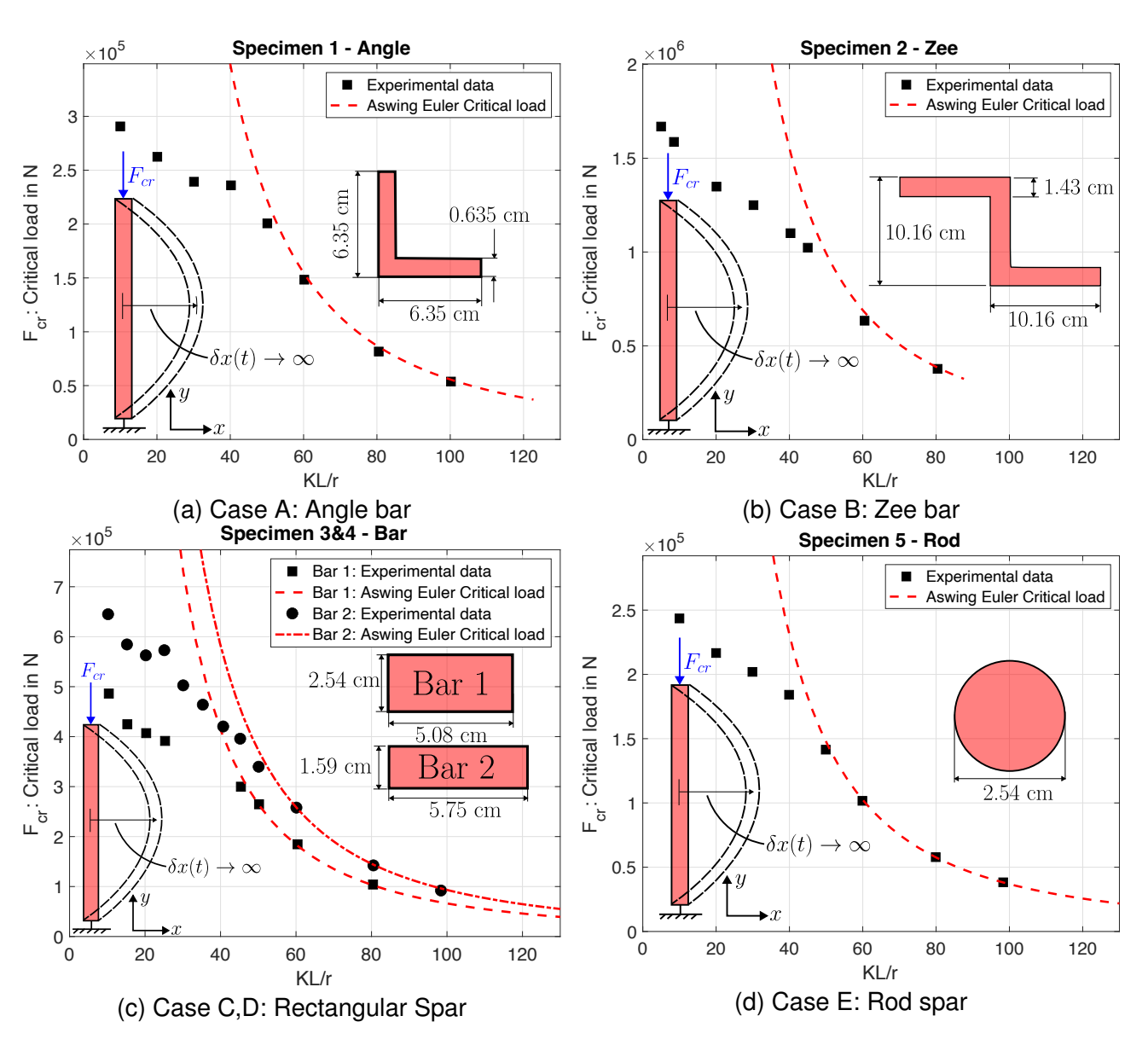


Figure 7 – Buckling cases A-E: Column buckling validation cases, with various cross section. Effect of the effective slenderness ratio KL/r (with K=0.5) on the critical load. Aswing expected predictions performance based on the Euler critical load solution. Experiments are from Niles' technical note [31].

6. Longitudinal and lateral behavior of folding wing tips

In this section, the capacity of Aswing to predict the behavior of Flared Folding Wingtips is assessed. To do so the experimental bench of Healy [17, 16] has been used. In his work, he has studied, the effect of the airspeed, angle of attack and sideslip angle on the behavior of three Flared Folding Wing Tips. Each of the bench have been reproduced numerically in Aswing to assess its prediction quality. **Experimental setup:**

The wing had a span of 1000 mm, a constant chord of 78 mm, untwisted shape, and a constant NACA0015 sectional profile as depicted in figure 9 (a) and (b). Regarding instrumentation, the model was equipped with an RLSRM08 encoder in both hinges, allowing fold angles to be measured. Testing was conducted in the 7ft by 5ft low-speed closed-return wind tunnel at the University of Bristol. The model was mounted to a six-components overhead balance, which, with the aid of a rear strut, could vary the angle of incidence of the model between -20 and +30 degrees and the side slip angle of the model between -/+ 50 degrees. In Healy's work, testing was broken into three stages but only the first one is of interest in this work that is the static behaviour of FFWTs with side slip angle, speed and angle of attack.

Numerical setup:

Healy's bench has been reproduced numerically. XFOIL analysis of the NACA0015 have been performed at the wind tunnel conditions, but are not presented here. All the mandatory geometric parameters are provided in Healy's manuscript [17] (chapter 7) leading to 3 separate Aswing input files.

6.1 Longitudinal and lateral behaviour of untwisted Flared Folding Wing Tips

In this section, we present a comparison between Aswing predictions, and the experiments of Healy for the case of the untwisted flared folding wingtip.

Variation of the coast angle θ with the airspeed:

The first series of measure performed by Healy is the variation of the coast angle θ (illustrated in figure 9) with the airspeed. The comparison with the Aswing predictions is presented in figure 8 (a) to (c) for 3 angles of attack and 3 flare angles. Aswing shows good agreements for the configurations with the flare angles of 20 and 30 degrees. The dispersion of accuracy is due to the NACA0015 Xfoil polars, that have been computed at a single Reynolds number. For the 10 degrees flare angle case, Aswing shows good agreement only at low speed.

Variation of the coast angle with the angle of attack: Healy proposed a refinement of his measurement at a single airspeed that is 22m/s. He has provided the variation of the coast angle against the angle of attack for each flare angle case. This time for the 3 cases, Aswing shows excellent agreement with the experiments as depicted in figure 9 (a). The 10 degrees flare case shows weaker prediction at high angle of attack, but they are still reasonable.

Variation of the coast angle with the side-slip angle:

Healy has proposed to study the sensitivity of the 20 degrees flare case to cross wind flow at 22m/s. We did so in Aswing, and the comparison is reported in figure 9 (b) where it shows good agreements with experiments for side slip angle not exceeding 20 degrees. For the angle of attack of -3 degrees, Aswing shows weaker predictions.

6.2 Effect of the wing tip twist

Healy has extended his work, to Folding Wing Tip having tip twist variation. Indeed as for most aeroplanes (such as the JWRA prototype) wingtips are usually twisted, so it is important to capture this effect. The latter is illustrated in figure 10(a). Two other benches were built having a -6 and a 9 degrees tip twist angle. Again he studied the effect of the side slip and incidence angles on the coast angle. Only the 20 degrees flare case was studied at 22m/s. Aswing predictions are compared to the experiments in figure 10 (a) and (b). In these two cases, the Aswing predictions quality decrease quite fast. We have even witnessed convergence issues for some cases, mostly due to the sharp change in the twist angle of the wingtip. However at zero sideslip angle, Aswing keep the same level of accuracy as the one of the previous subsection. In the case of this paper methodology, only the zero side slip angle is of interest, and here the level of accuracy of Aswing for every bench presented is more than satisfying.

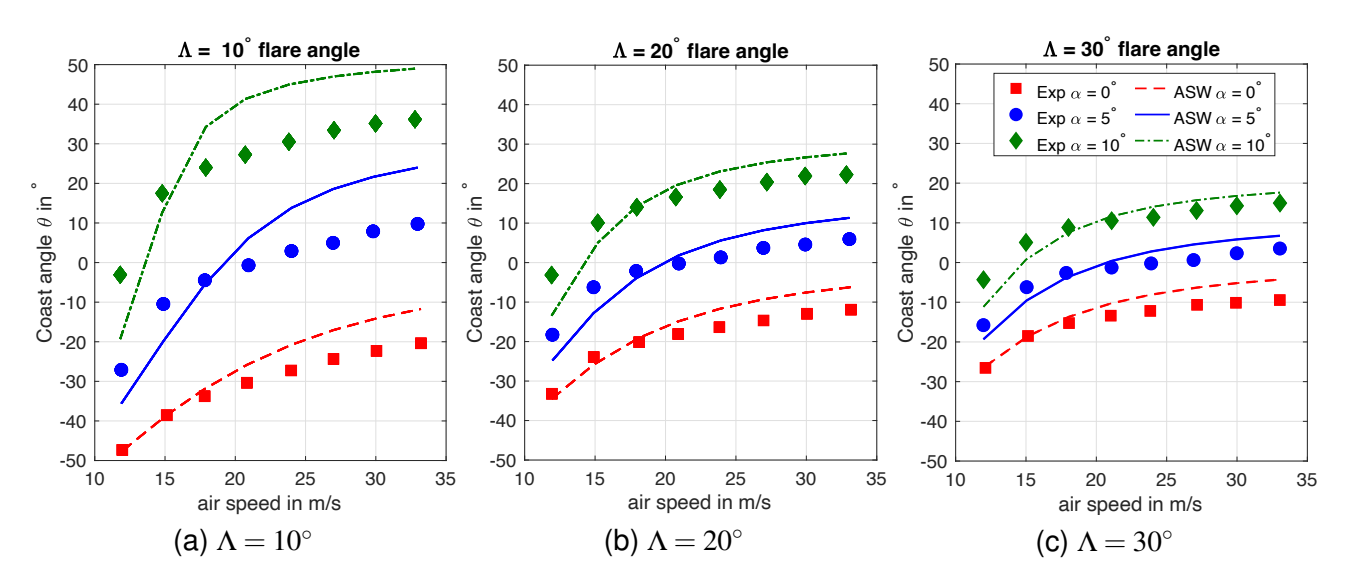


Figure 8 – Effect of the flare angle Λ , angle of attack and airspeed on the wingtip coast angle θ . Comparison of the Aswing predictions with the experimental data from Healy's work [16].

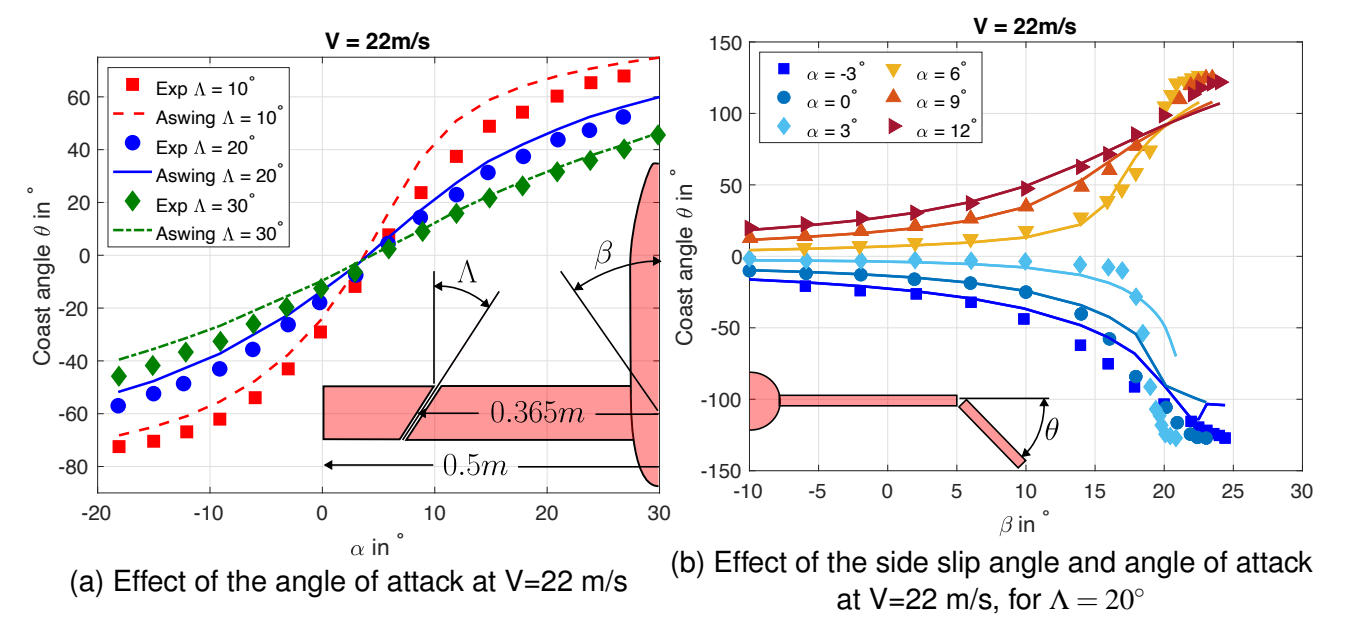


Figure 9 – Sensitivity study of the lateral and longitudinal characteristic of Healy's bench to incidence and sideslip angles. Aswing predictions against experiments from Healy [16].

On the real effect of Flared Folding Wing Tips:

The coast angle is not really a measure, of the load alleviation provided by the Flared Folding Wing Tip. However, we have shown previously [25] that Aswing captures well the impact of various wingtip devices on the lift and drag of wings. As the root bending moment is mostly the lift integrated along the span, and by showing that Aswing captures well the variation of the coast angle with various parameters, it will captures well their effect on the root bending moment.

In conclusion, in this section we have shown that Aswing is able to capture the static behavior of Flared Folding Wing Tips with various parameters (side slip, angle of attack, speed, flare angle, tip twist). In light of the previous section, it can be used for the simultaneous analysis of joined wing with folding wingtips.

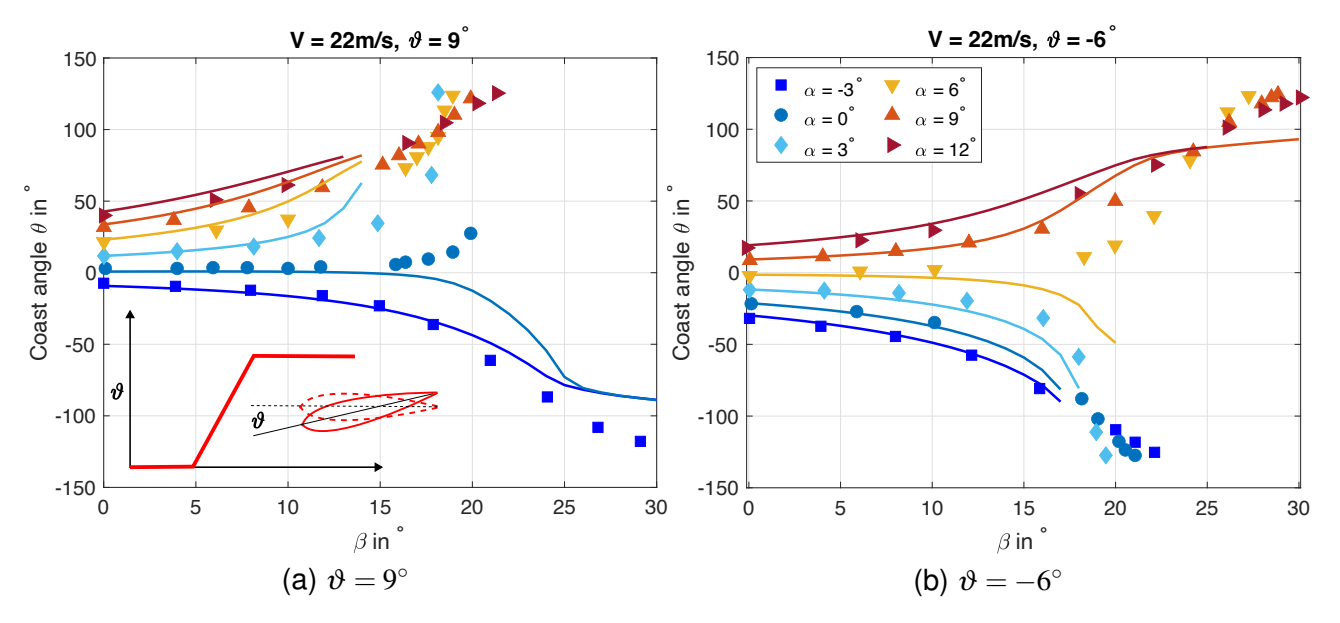


Figure 10 – Effect of the wing-tip twist distribution on the performance of the folding wingtip. Variation with the angle of attack and side slip angle. Aswing predictions versus experiments from Healy's work [16]. Lines stops before first convergence failure. Tests were done for $\Lambda=20^\circ$ and V=22m/s.

7. Structural performance of the JWRA with Flared Folding Wing Tips

7.1 Sizing problem:

In this section, the performance gains brought by folding wing-tips on a joined wing layout are discussed. The Nasa-JWRA-JW1 prototype has been retained as this section application example, mostly because we have shown good Aswing prediction performances for both aerodynamic and structural analysis. In this example, the folding wingtip hinge is placed at the joint location. In total 4 hinge angles have been tested that are $\Lambda = 0.10, 20, 30^{\circ}$. Bigger values have not been taken, as we wanted to remain in the range of precision ensured by the evaluation presented in the previous section. The aircraft speed was set up at 130ft/s ensuring a 12lb lift, that is the prototype weight. Then, the angle of attack was changed to ensure a 2.5G load factor ($\alpha = 2.86^{\circ}$). In this configuration, the rear wing carries 20% of the total load. The effect of the folding wing tip on the shear loads and bending moment distributions are presented in figure 11 (a) to (f). No matter the hinge angle, the folding wingtips provide an important load relief specially on the inboard sections. For example, the forward wing root bending moment is reduced by up to 40%. The normal shear stress force, is also reduced by 12%. Also, the normal bending moment is reduced by up to 60% as well as the torsional moment. Finally the extensional load is reduced by 50%. Overall, the hinge angle of $\Lambda = 0^{\circ}$ provides the most promising results. However, it is important to check if the flap placed on the folding wingtip will be powerful enough to bring back the wing tip in its initial position during cruise. Such analysis can be performed in Aswing but it is not presented here. For the sizing methodology average values of the gains are taken.

7.2 Mass saving estimation

From the previous sub-section, the folding wingtips provide significant load reduction, thus an estimation of the mass saved on the structure is proposed using TASOPT wing box methodology [33]. Here the caps and webs of the rear and forward wing are not directly computed. Instead, a relative comparison is proposed based on the load alleviation observed in the previous section. According to Drela [33], the design of a joined wing structure can be separated into 3 parallel wing box design. In this work, the TASOPT wing box model is adopted. In the latter, only the webs and caps thickness are the parameters of design.

1- Outboard section: Folding wing tip.

The wingtip can be considered as a simple cantilever wing. According to Drela [33], if the wingtip has a triangular chord distribution which is the case of the JWRA wingtip, the web and caps thickness scales respectively as follows:

$$t_{web,j} \propto F_{n,j} \tag{2}$$

$$t_{cap,j} \propto (M_{c,i})^{1/3}$$
 (3)

where $F_{n,j}$ and $M_{c,j}$ are the normal shear load and out of the plane bending moment at the j-oint location, ie 60% of the half span here. The exact solution for $t_{web,j}$ and $t_{cap,j}$ are provided in Drela's work [33], and are dependant of geometric parameters, that do not vary from the case with and without folding wingtips, thus they have been omitted for each of the following equations to come. The relative thickness change of the caps and webs can be expressed as:

$$\frac{t_{web,j,FWT}}{t_{web,j}} = \eta_{F_{n,j}} \tag{4}$$

$$\frac{t_{web,j,FWT}}{t_{web,j}} = \eta_{F_{n,j}}$$

$$\frac{t_{cap,j,FWT}}{t_{cap,j}} = (\eta_{M_{c,j}})^{1/3}$$
(5)

where η_{F_n} and η_{M_c} are the shear and bending moment relief due to the use of folding wing-tips. From figure 11 (a) and (f) η_{F_n} and η_{M_c} can be identified. In this case, $\eta_{F_n} = 0.24$ and $\eta_{M_c} = 0.17$. So here, the folding wingtip wingbox can not be designed based on the 2.5G load case, as in the clamped case (cruise condition - 1G, where the folding wingtip are fixed) the shear and bending moment are more important. Thus η_{F_n} and η_{M_c} are fixed to 0.6 which is the ratio of the 1.5G/2.5G condition. 1.5G is still reasonable to provide the aircraft good manoeuvrability performances.

2- Forward wing Inboard section:

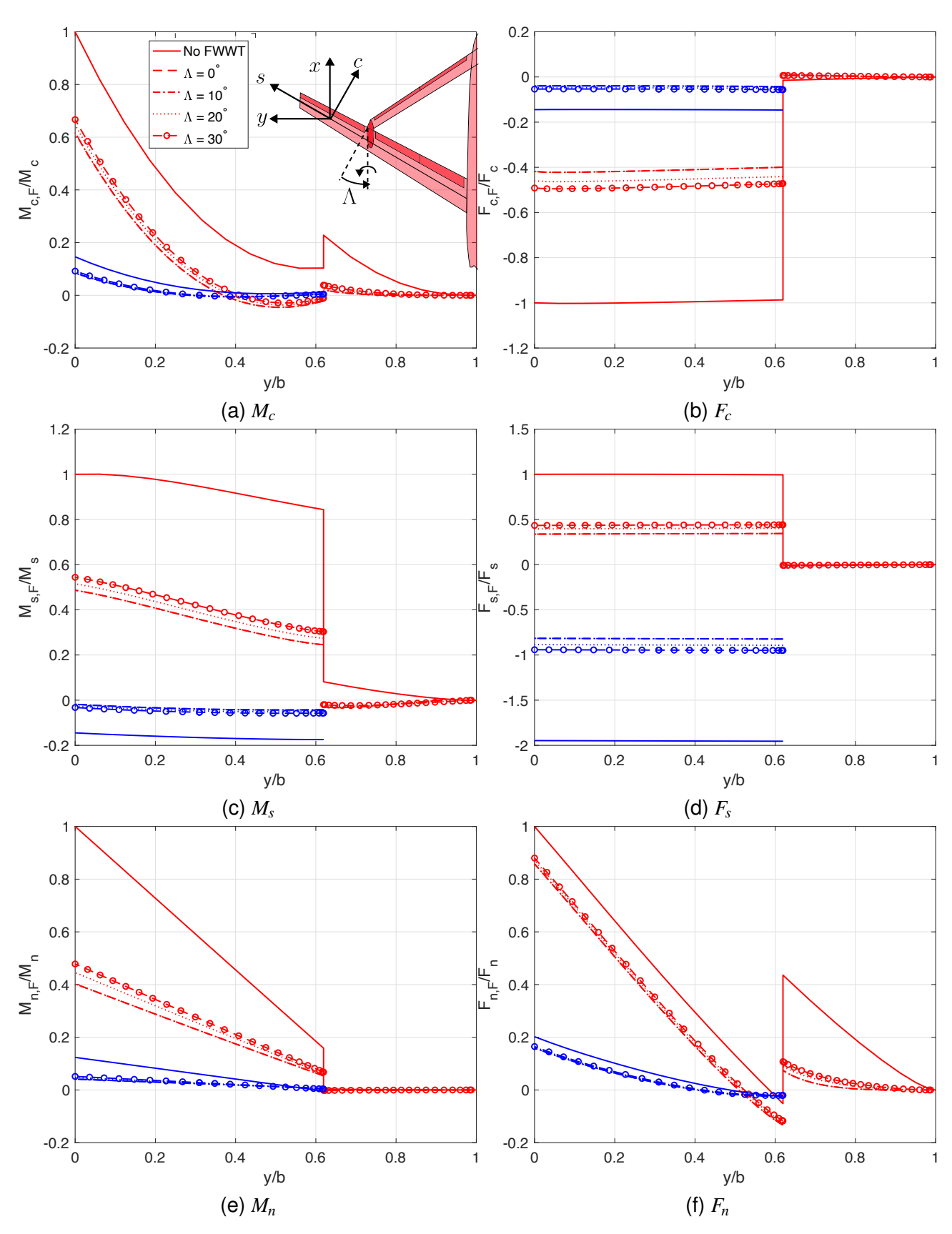


Figure 11 – JWRA with Flared Folding Wing Tip. Effect of the hinge angle on the rear wing (in blue) and the forward wing (in red) loads. Shear loads and moments are given as a fraction of the values of the JWRA without folding wingtips.

As it has been identified in figure 11 the rear wing provides an important relief in the inboard bending moment and shear loads. Despite, this configuration could be considered as a strut braced wing, the load relief brought by the rear wing, is more close to the one brought by an engine anchored at the joint location. Thus according, to Drela [33], in this configuration, the forward wing inboard section wing box caps and webs thickness scales as follows:

$$t_{web,r} \propto F_{n,r} \tag{6}$$

$$t_{cap,r} \propto (M_{c,r})^{1/3} \tag{7}$$

where $F_{n,r}$ and $M_{c,r}$ are the normal shear load and out of the plane bending moment at forward wing r-oot. The relative thickness change of the caps and webs can be expressed as:

$$\frac{t_{web,r,FWT}}{t_{web,r}} = \eta_{F_{n,r}} \tag{8}$$

$$\frac{t_{cap,r,FWT}}{t_{cap,r}} = (\eta_{M_{c,r}})^{1/3} \tag{9}$$

where η_{F_n} and η_{M_c} are the shear and bending moment relief due to the use of folding wing-tips. From figure 11 (a) and (f) η_{F_n} and η_{M_c} can be identified. In this case, $\eta_{F_{n,r}} = 0.88$ and $\eta_{M_{c,r}} = 0.61$, both are above 0.6 (1.5G maneuver case).

3 - Rear wing section:

On a joined wing, the rear wing works in compression, so Drela's work [33] on strut-braced wing cannot be invoked here. Also usually in compression, column buckling occurs before, static failure, so the maximum strain constraint can not be used to design the rear wing box. Instead, the Euler ultimate buckling load constraint is used to design the caps thickness, as they provide the weakest bending stiffness. In other word, according the rear wing box shape, the buckling will necessary occur in the normal direction (out of the plane), so the caps thickness is the critical parameter here. According to the ultimate load expression (cf section V) the caps thickness scales as follows

$$t_{cap} \propto (F_s)^{1/3} \tag{10}$$

where F_s is taken arbitrary along the rear wing span as it is constant (cf figure 11-d). The cap thickness ratio between the case with and without folding wingtip is given as follows:

$$\frac{t_{cap,r,FWT}}{t_{cap,r}} = (\eta_{F_s})^{1/3} \tag{11}$$

where η_{F_s} is the extensional stress relief due to the folding wing tip. In this case, $\eta_{F_s} = 0.48$ so again, its value must be rise to 0.6 to match the 1.5G maneuver condition.

For the rear wing web thickness design, the load distribution follows the same shape as the outboard section, so the web thickness scales as follows:

$$t_{web,r} \propto F_{n,r} \tag{12}$$

where $F_{n,r}$ is the root normal shear force of the rear wing. It comes finally the rear wing web thickness ratio as follows:

$$\frac{t_{web,r,FWT}}{t_{web,r}} = \eta_{F_{n,r}} \tag{13}$$

where in this case $\eta_{F_{n,r}} = 0.8$.

Total mass saving estimation:

From the equations above it is possible to compute the total structural mass saving due to the use of folding wingtip. Each of the equations, provide a thickness saving that must translated into a mass one. And each mass saving must be weighted by real weight of each elements composing the joined wing. The mass of the webs and caps are given by their area times their density (here equal) integrated along each lifting surface span. Lets introduced $\eta_{web} = A_{web}/A_{box}$ and $\eta_{cap} = A_{cap}/A_{box}$, that represent the area weight of the caps and webs on each wing box. According to Stearman

[11] and Lin [10] data, $\eta_{web}=0.25$ and $\eta_{cap}=0.75$. Two other weight ratios must be introduced, that are $\eta_{FW}=m_{FW}/m_{FW+RW}$ and $\eta_{RW}=m_{RW}/m_{FW+RW}$. They represent the weight ratio of the forward and rear wing. Again from the bench data, $\eta_{FW}=0.7369$ and $\eta_{FW}=0.2631$. Finally 2 last weighting parameters must be introduced that are $\eta_{FW,I}=0.8384$ and $\eta_{FW,O}=0.1616$, that weight the mass between the forward wing inboard and outboard section. The structural mass saving due to the use of folding wingtip is then given by:

$$\eta_{M} = \eta_{FW} \left(\eta_{web} (\eta_{FW,I} \eta_{F_{n,r}} + \eta_{FW,O} \eta_{F_{n,j}}) + \eta_{cap} \left(\eta_{FW,I} (\eta_{M_{c,r}})^{1/3} + \eta_{FW,O} (\eta_{M_{c,j}})^{1/3} \right) \right) \\
+ \eta_{RW} \left(\eta_{web} \eta_{F_{n,r}} + \eta_{cap} (\eta_{F_{s}})^{1/3} \right)$$
(14)

When the above numerical values are used, the use of folding wing tips brings a mass saving of 14.2% ($\eta_M = 0.8579$). Now according to Wolkowitch, when asymatric wing box is used on joined wing to take the maximum benefit of the in the plane bending stiffness, a joined wing without folding wing tip can have a mass 40% lower than the one of a cantilever plus horizontal stab configuration. If folding wingtip are considered to be used, the mass saving would drop to 48.53%.

7.3 Breguet analysis and extension to existing transport aircraft

In this sub-section, a Breguet analysis is proposed, to assess the energy consumption saving brought by the use of a joined wing configuration with folding wingtip in comparison to the classical trapezoidal swept back wing with an horizontal stab. As an important reminder, the JWRA-JW1 provides the same aerodynamic performances as the cantilever wing and the same longitudinal stability (static margin). This analysis is applied to a representative fleet from short to long range mission (Embraer 195, Boeing 737-800 and Boieng 777-300).

The range of an aircraft can be reasonably approximated by the Breguet equation as follows:

$$Range = \frac{V}{g} \left(\frac{CL}{CD} \right) I_{sp} ln \left(\frac{W_I}{W_F} \right) \tag{15}$$

where V, $\frac{CL}{CD}$, I_{sp} are respectively, the flight speed, the aircraft lift-to-drag ratio, and the engine specific impulsion in cruise and are reasonably supposed to be fixed from a configuration to another. W_I and W_F in the above equation are, the initial and final weight of the aircraft. W_I is the sum of the fuel weight, payload and empty weight. When mass is saved on some component of the aircraft, it induces a reduction of the empty weight. Assuming V, $\frac{CL}{CD}$, I_{sp} are held constant, 6 scenarios can be derived from the Breguet analysis to assess the performances gains.

Scenario I: Increase PAX, ISO Fuel, ISO Range, ISO MWTO

The mass saved on the joined wing is used to increase the number of passengers on each aeroplanes. As the current fuselage are designed for the maximum passengers already, the mass saved must penalised to account for the bigger fuselage sizing, extra fuel consumption resulting from extra drag. In consequence by denoting M_{PAX} the mass of a passenger and its luggage (125 kg to be conservative), and by denoting ΔW_{JW} the mass saving brought by the joined wing with or without flared folding wingtips, the extra number of PAX ΔN_{pax} can be expressed as

$$\Delta N_{pax} = \eta_{penalty} \frac{\Delta W_{JW}}{M_{PAX}} \tag{16}$$

where $\eta_{penalty}$ stands for the mass penalty applied to each PAX for the extra fuselage section. According to Wolkovitch, a value of 0.7 is reasonable but 0.5 was also picked to be very conservative. In this scenario, the aeroplane takeoff at the same maximum operating weight than the conventional layout and fulfill the same mission but with more passenger. The gain in energy consumption per unit of payload per unit of distance flew (denoted as PFEI) is thus obtained by the equation below

$$\eta_{PFEI} = \frac{N_{pax}}{N_{pax} + \Delta N_{pax}} \tag{17}$$

Scenario II: Increase PAYLOAD, ISO Fuel, ISO Range, ISO MWTO

This scenario is more attractive than the first as we can take more benefit of the mass saved. Here

the aeroplane is assumed to fly in a freighter mode. In this case, the mass saved is fully transformed into payload (cargo). The cargo density of each case will be commented later. Thus then gain in PFEI is directly given by

 $\eta_{PFEI} = \frac{M_{PAYLOAD}}{M_{PAYLOAD} + \Delta W_{IW}} \tag{18}$

where $M_{PAYLOAD}$ is the payload mass of the classical layout. Thus in this scenario, the aircraft with joined wing has the same Maximum takeoff, carry the same fuel and fly over the same distance than the classical layout but with an extra cargo.

Scenario III: Extra Range ISO fuel, iso PAX reduced weight

In this scenario, the extra range brought by the use of joined wing being lighter is assessed for the same quantity of fuel and PAX carried. The extra range can be obtained from the Breguet formula as follow

$$\eta_{R,JW} = \frac{ln\left(\frac{W_{I,JW}}{W_{F,JW}}\right)}{ln\left(\frac{W_{I}}{W_{F}}\right)} \tag{19}$$

where $W_{I,JW}$ and $W_{F,JW}$ are the initial and final mass of the joined wing configuration embedding the mass savings. Follow immediately the gain in PFEI as follow

$$\eta_{PFEI} = \frac{1}{\eta_R} \tag{20}$$

Scenario IV: Max Range extended fuel, iso PAX, MAX Takeoff Weight

As reported by Wolkovtich a major benefit brought by joined wings is the bigger tanks they offer. Indeed on this type of layout the rear wing is carrying fuel, which is not the case for conventional layouts (not true for A380 and B747). Moreover, joined wings can take benefit of larger wing boxes ie tanks. In consequence according to Wolkovitch, joined wings can carry 50% more fuel than conventional layouts. We will take this value as a reference in the remaining part of this paper. Thus the mass saved is completely transformed into fuel to perform a longer mission. The gain in fuel is expressed by

$$\eta_{fuel,JW} = \frac{W_{fuel} + \Delta W_{JW}}{W_{fuel}} \tag{21}$$

and the extended range is provided from Scenario III equation, leading to the gain in PFEI as follows.

$$\eta_{PFEI} = \frac{\eta_{fuel,JW}}{\eta_{R,JW}} \tag{22}$$

In other word, this scenario is an extension of the third one with more fuel in the wings. The aircraft takes off at Maximum Weight.

Scenario V: Fuel Saving at Design Point

As the joined wing is lighter than the conventional layout, less fuel can be used to performed the same design mission. The fuel saved can be computed from the Breguet equation leading directly to the gain in PFEI.

$$\eta_{PFEI,JW} = \eta_{fuel,JW} \tag{23}$$

In this scenario the airplane is not flying at the Maximum Takeoff Weight which is the case of the conventional layout.

Scenario VI: Ultimate range with or without bigger tanks

In this scenario, the ultimate range of the airplane is estimated with and without the bigger tank. The payload is set to zero. The gain in range is computed from the Breguet analysis, with the fuel set up to never exceed the tank capacity or the Maximum Takeoff weight of the airplane. The gain in PFEI is not computed here as no payload is carried. The gain of performances is thus measured through $\eta_{R,JW}$ only.

For each of the scenario presented the gain brought by the joined wing alone is denoted with the subscript JW while the joined wing with FFWT by JW + FFWT.

For each scenario, the mass of the horizontal tail, wings and fuel are needed to assess the performances brought by joined wing with or without FFWT. Unfortunately, except for fuel, these quantities are not publicly available. To estimate each component mass fraction on our fleet example's aircrafts that are B737-200 and 800, Boeing 777-300 and Embraer E-195, TASOPT ([33, 34, 35, 36] has been used. To make sure it was providing realistic one, a validation of the software has been performed on public data that are, empty weight, max fuel weight and maximum takeoff weight. This validation is summarized in table 1. The maximum prediction error for the Maximum Takeoff weight is below error, while for the Fuel at design point is below 9.1% and for the empty weight is below 9.9%. The Boeing 777-300 is the worst case, for the remaining aeroplanes the prediction error is below 3% making TASOPT a reliable framework. Each components masses and the mass saving brought by joined wings with or without Flared Folding Wing Tips are summarized in table 2. Using the latter, the performances gains for each scenario could be then evaluated and are summarized in table 3. From every scenario, the ones that brings the most reduction in PFEI are the first and second that is a conversion of the mass saved into Payload, with a PFEI reduction up to 25,9 % for extra PAX and 33,3% for extra cargo. Both the joined wings and FFWT bring significant improvements with a bigger contribution from the joined wings layout. From Scenario IV and VI, the bigger tank available on the joined wing allows a significant extension of the payload range as illustrated in figures 12 (a) and (b) for the Embraer E195 and Boeing B777-300. Also the benefit brought by the joined wing with FFWT increase with the mission range (cf table 3) because the wing and horizontal masses account for a bigger amount of the aircraft empty weight (cf table 2 with $\eta_{Wing+HT}$).

It is important to temper these performance results in light of the methodology used in this work. First of all, the wing box sizing method is based on loads in steady condition. Nevertheless, Healy has shown, that the load alleviation provided by folding wingtips varies quite a lot with the gust frequency (chapter 7 of [17]. Secondly, the wing box methodology is quite coarse. A more sophisticated approach could bring better insight on the structural sizing. Finally, the Breguet analysis can be improved by integrating the complete aircraft mission. Aswing has shown promising performances prediction of joined wing with folding wing-tips, it must be now integrated into an OAD framework, such as FASTOAD to provide more sophisticated design analysis. The main goal being to shrink each aircraft's extended range to the original one, but for that the wing surface must be reduced (because of the mass saved) and so the analysis must loop on the mass to get a new MTOW at the design mission, which is not possible with the Breguet analysis alone.

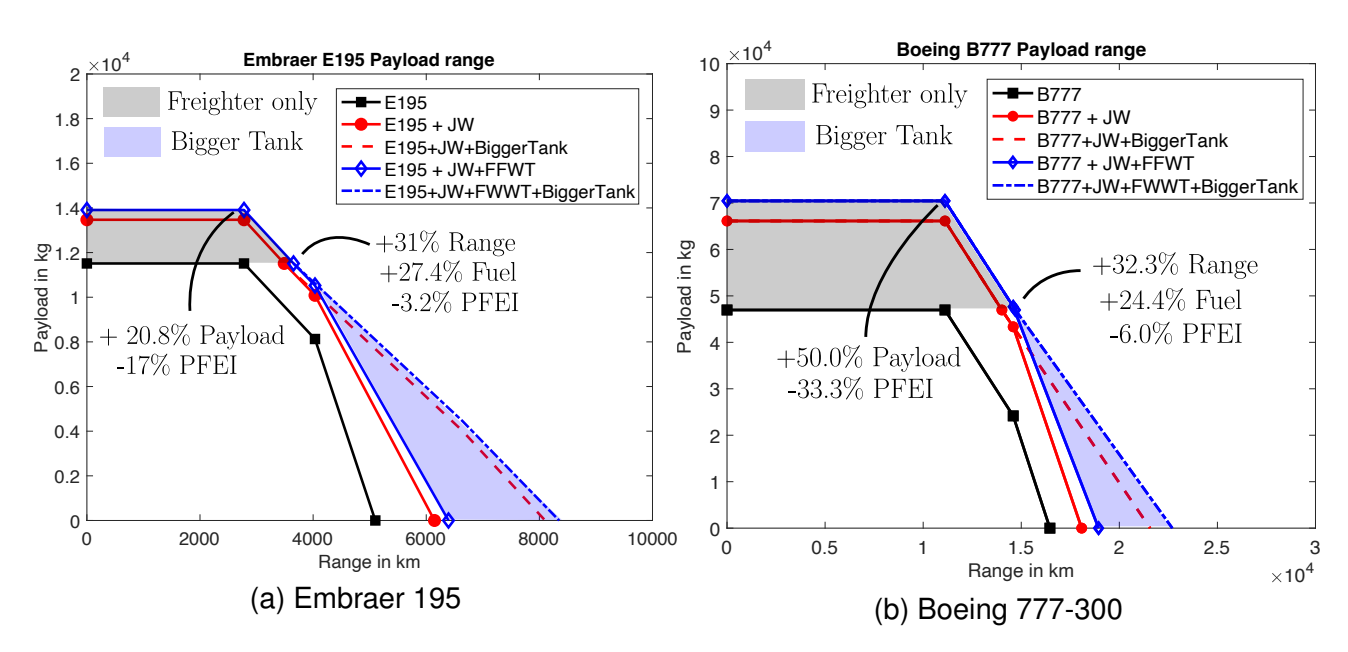


Figure 12 – Extended Payload range from the Breguet analysis with classical layouts replaced by wings w/wo Flared Folding Wingtips

	E195	B737-200	B737-800	B777-300
MTOW TASOPT (in kg)	48191	56630	75296	286740
MTOW Real (in kg)	48790	55340	77564	28700
MTOW error in %	-1.2	2.3	-2.9	-0.4
Wfuel TASOPT (in kg)	NC	18362	17451.5	148224.3
Wfuel real (in kg)	NC	18170	17690.1	135880
Wfuel error in %	NC	1.1	-1.3	9.1
Wempty TASOPT in kg	26558.9	26560.5	40268.3	142066
Wempty real (in kg)	28700	27170.2	44412.9	157759.3
Wempty error (in %)	-7.5	-2.2	-2.8	-9.9

Table 1 – TASOPT [33] validation upoon real airport data [37, 38, 39], on 4 different transport aero-planes

Aircraft	Units	E195	B737-200	B737-800	B777-300
W_{PAY}	kg	11512,2	11707,2	17560,8	46965,4
W_f	kg	8755,7	18361,9	21539,7	96268,6
$W_{OE} = W_{Empty} + W_{Payload}$	kg	36880,2	38267,7	57828,9	187229,6
W_{wing}	kg	4359,0	5967,5	10757,8	45299,8
W_{HT}	kg	529,8	627,9	1186,6	2651,1
$\overline{W_{Wing+HT} = W_{Wing} + W_{HT}}$	kg	4888,7	6595,4	11944,5	47950,8
$\eta_{HT+W} = W_{Wing+HT}/W_{Empty}$	%	19,3	24,8	29,7	34,2
ΔW_{JW}	kg	1955,5	2638,1	4777,8	19180,3
$\Delta W_{JW+FFWT}$	kg	2395,5	3231,7	5852,8	23495,9

Table 2 - Aircraft mass breakdown (data from TASOPT), mass saved using joined wing w/wo Flared Folding Wing Tips

Scenario I : Increase P					D777 000	Mana
Aircraft	Units	E195	B737-200	B737-800	B777-300	Mass penalty η_p
$\eta_{PAX,JW}$	<u>%</u>	8,5	11,3	13,6	20,4	0,5
• ,	%	11,9	15,8	19,0	28,6	0,7
$\eta_{P\!AX,JW+FWWT}$	%	10,4	13,8	16,7	25,0	0,5
	%	14,6	19,3	23,3	35,0	0,7
$\eta_{PFEI,JW}$	%	-7,8	-10,1	-12,0	-17,0	0,5
	%	-10,6	-13,6	-16,0	-22,2	0,7
$\eta_{PFEI,JW+FWWT}$	<u>%</u>	-9,4	-12,1	-14,3	-20,0	0,5
	%	-12,7	-16,2	-18,9	-25,9	0,7
Scenario II : Increase C	Cargo Pa	yload, I	SO fuel, ISC	Range ISO	MWTO	
V_{cargo}	m^3	102	77	150	766	
$\eta_{PAYLOAD,JW}$	%	17,0	22,5	27,2	40,8	•
$\eta_{PAYLOAD,JW+FWWT}$	%	20,8	27,6	33,3	50,0	-
$\eta_{PFEI,JW}$	%	-14,5	-18,4	-21,4	-29,0	-
$\eta_{PFEI,JW+FFWT}$	%	-17,2	-21,6	-25,0	-33,3	-
$\rho_{cargo,JW}$	kg/m^3	132,0	186,3	148,9	86,4	-
$\rho_{cargo,JW+FWWT}$	$kg/^3$	136,3	194,0	156,1	92,0	-
Scenario III : Extra Ran	ige ISO	Fuel ISC	PAX, reduc	ed weight		
$\eta_{R,JW}$	%	5,0	6,1	7,6	9,2	
$\eta_{R,JW+FFWT}$	%	6,2	7,5	9,5	11,5	
$\eta_{PFEI,JW}$	%	-4,8	-5,7	-7,1	-8,4	-
$\eta_{PFEI,JW+FFWT}$	%	-5,9	-7,0	-8,7	-10,3	-
Scenario IV : Extra Rar	nge ISO	PAX ISC) MWTO			
$\eta_{fuel,JW}$	%	22,3	14,4	22,2	19,9	
$\eta_{fuel,JW+FFWT}$	%	27,4	17,6	27,2	24,4	-
$\eta_{R,JW}$	%	25,6	18,2	27,2	26,1	-
$\eta_{R,JW+FFWT}$	%	31,5	22,5	33,7	32,3	-
$\eta_{PFEI,JW}$	%	-2,6	-3,3	-4,0	-4,9	-
$\eta_{PFEI,JW+FFWT}$	%	-3,2	-4,0	-4,9	-6,0	-
Scenario V : Fuel Savir						
	%	-7,7	-9,9	-21,9	-23,7	
$\eta_{S,JW}$	/ %	-9,4	-12,2	-14,5	-16,8	-
$\eta_{S,JW+FFWT}$	/ %	-5,3	-6,9	8,3	-10,0	-
$\eta_{fuel,JW}$	<u> </u>	-6,5	-8,4	-10,1	-10,2	-
$\eta_{fuel,JW+FFWT}$	% %	- 0,5 -5,3	-6, 4 -6,9	8,3	-12,5	-
$\eta_{PFEI,JW}$		-6,5	-8,4	-10,1	-10,2	-
η _{PFEI,JW+FFWT}			· · · · · · · · · · · · · · · · · · ·			
Scenario VI : Ultimate						
$\eta_{Range,JW,normal\ tank}$	%	+20,5	NC	+16,2	+23,9	
$\eta_{Range,JW+FFWT,normal\ tank}$	%	+25,3	NC	+20,0	+29,8	-
$\eta_{Range,JW,bigger\ tank}$	%	+58,8	NC	+53,9	+32,4	-
$\eta_{Range,JW+FFWT,bigger\ tank}$	%	+63,7	NC	+57,7	+39,7	

Table 3 – PFEI improvement brought by the use of joined wing w/wo Flared Folding Wing Tips on 6 different scenarii

Comments on the computational time performances This section is ended with a short comment on the computational performance of Aswing on the series of analysis performed in this paper. In total 5 different calculations have been performed. 1 - Compute a polar of a configuration, 2 - Compute the static response of a configuration, 3 - Perform a bluckling analysis (static response + modal analysis), 4 - Compute the response of a folding wing tip to a set of parameters, 5 - Trim a configuration and find the angle of attack satisfying a 2.5G load (2 trim problems). The computational performances are summarized in the table 4. The tests were done on Macbook Air M2. As highlighted every analysis performed in this paper have run in less than a second, making Aswing a promising multidisciplinary analysis tool.

Operation	Computational time (in seconds)
1	0.200 * N _α
2	0.200
3	1.0
4	0.200
5	0.400

Table 4 – Computational performance for each operation performed in this paper. N_{α} is the number of points to be computed in the polar.

These relatively low computation times make it feasible to directly call ASWING in OAD processes and ultimately at different design points. A Python wrapper for ASWING has been implemented with an acceptable level of parametrization, without compromising computational performance. Future work will focus on identifying relevant interfaces and process logic for integration into FAST-OAD, aiming to fully exploit the promising capabilities of ASWING.

8. Conclusion

In this paper, an experimental evaluation of Aswing for the aeroeastic analysis of joined wing with flared folding wing tips (FFWT) has been proposed. Then, as a test case of the Aswing robustness, a study on the effect of FFWT on the structural performances of a joined wing prototype and its real gain on fuel consumption followed. The main results are summarized as follows:

- Aswing predicts well the longitudinal aerodynamics of the joined wing, especially for lift and drag. For the pitching moment, the predictions are reasonably good and can be easily improved with a small modification of the code.
- Aswing predicts well the structural response of a joined wing. It also captures well the effect of introducing some degrees of freedom from the joints.
- Aswing, can natively predict the buckling of a complex platform such as a joined wing. It will give good results as long as the slenderness ratio of the structure is above 50.
- Aswing, can predict the longitudinal and lateral behavior of flared folding wing tips, with a flare angle up to 30°. It shows convergence problems, for side slip angles above 20°. Finally, it captures the effect of twist spanwise distribution on the above phenomena.
- In light of this evaluation, Aswing has been used on an application example, showing that flared folding wing tip used on a joined wing could lead to a reduction of its mass by 14.2%. The use of a joined wing with Flared Folding Wing Tip could provide in consequence a mass saving of 48.5% in comparison to a classical swept back wing with an horizontal tail for the same aerodynamic performances
- From a Breguet analysis, a joined wing could bring between 6.5 to 12.5 % fuel savings compared to conventional layouts for the same design mission. If the Paylaod is extended, the gain in PFEI varies from 17,2 to 33,3%. Thanks to bigger tanks, this layout can carry the same

design between 31,5 and 32,3% further. The airplanes ultimate range is increased between 32,43% and 63,7%. The gain increases with the payload range product of the aircraft. For larger airplanes, the wing and horizontal stabilizer masses account for a greater proportion of the structure aircraft mass, increasing the benefit brought by the joined wing and Flared Folding Wing tips.

In conclusion, this paper has shown through its methodology that joined wings with flared wingtips are a good lever to reduce fuel consumption of next generation aircraft. However, this type of analysis needs to be integrated into more sophisticated overall aircraft design frameworks such as FAST-OAD to better assess the benefits and possible constraints. This will allow more rigorous conclusions to be drawn about these promising unconventional configurations.

9. Contact Author Email Address

The data presented in this paper can be obtained on demand. Please contact the main author of this paper using the following email-adress: romain.jan@isae-supaero.fr

10. Copyright Statement

The authors (R.Jan, S. Delbecq and E. Benard) confirm that they, and/or their company or organization (ISAE-Supaero), hold copyright on all of the original material included in this paper. The authors also confirm that they have obtained permission, from the copyright holder of any third party material included in this paper, to publish it as part of their paper. The authors confirm that they give permission, or have obtained permission from the copyright holder of this paper, for the publication and distribution of this paper as part of the ICAS proceedings or as individual off-prints from the proceedings.

11. Acknowledgement

The authors would like to thank Dr Fintan Healy and the university of Bristol (UK) for sharing their experimental data on flared folding wingtips.

References

- [1] Delbecq, S, Fontane, J, Gourdain, N, Planès, T, and Simatos, F. "Sustainable aviation in the context of the Paris Agreement: A review of prospective scenarios and their technological mitigation levers". In: *Progress in Aerospace Sciences* 141 (2023), p. 100920.
- [2] Bravo-Mosquera, Pedro D, Catalano, Fernando M, and Zingg, David W. "Unconventional aircraft for civil aviation: A review of concepts and design methodologies". In: *Progress in Aerospace Sciences* 131 (2022), p. 100813.
- [3] Yutko, Brian M, Titchener, Neil, Courtin, Christopher, Lieu, Michael, Wirsing, Larry, Tylko, John, Chambers, Jeffrey T, Roberts, Thomas W, and Church, Clinton S. "Conceptual design of a D8 commercial aircraft". In: 17th AIAA Aviation Technology, Integration, and Operations Conference. 2017, p. 3590.
- [4] Ma, Yiyuan and Elham, Ali. "Designing high aspect ratio wings: A review of concepts and approaches". In: *Progress in Aerospace Sciences* 145 (2024), p. 100983.
- [5] Faggiano, Francesco, Vos, Roelof, Baan, Max, and Van Dijk, Reinier. "Aerodynamic design of a flying V aircraft". In: *17th AIAA Aviation Technology, Integration, and Operations Conference*. 2017, p. 3589.
- [6] Gagnon, Hugo and Zingg, David W. "Aerodynamic optimization trade study of a box-wing aircraft configuration". In: *Journal of Aircraft* 53.4 (2016), pp. 971–981.
- [7] Drela, Mark. "Integrated simulation model for preliminary aerodynamic, structural, and control-law design of aircraft". en. In: 40th Structures, Structural Dynamics, and Materials Conference and Exhibit. St. Louis,MO,U.S.A.: American Institute of Aeronautics and Astronautics, Apr. 1999. DOI: 10.2514/6.1999-1394. URL: https://arc.aiaa.org/doi/10.2514/6.1999-1394 (visited on 11/23/2022).

- [8] Wolkovitch, Julian. Low-Speed Wind Tunnel Test on Joined Wing and Monoplane Configurations. Volume 2. Test Data. Tech. rep. Nasa contractor report N00014-79-C-0953 or ACA Report 82-2. NASA, 1982.
- [9] Kroo, Ilan, Gallman, John, and Smith, Stephen. "Aerodynamic and structural studies of joined-wing aircraft". In: *Journal of aircraft* 28.1 (1991), pp. 74–81.
- [10] Lin, Hung-Hsi, Jhou, Jitai, and Stearman, Ronald. "Influence of Joint Fixity on the Structural Static and Dynamic Response of a Joined-Wing Aircraft: Part I: Static Response". In: *SAE Transactions* (1989), pp. 221–234.
- [11] Stearman, Ronald. "Influence of joint fixity on the aeroelastic characteristics of a joined wing structure". In: *31st Structures, Structural Dynamics and Materials Conference*. 1990, p. 980.
- [12] Castrichini, Andrea, Hodigere Siddaramaiah, Vijaya, Calderon, DE, Cooper, Jonathan E, Wilson, Thomas, and Lemmens, Yves. "Nonlinear folding wing tips for gust loads alleviation". In: *Journal of Aircraft* 53.5 (2016), pp. 1391–1399.
- [13] Castrichini, Andrea, Siddaramaiah, V Hodigere, Calderon, Dario E, Cooper, Jonathan E, Wilson, Thomas, and Lemmens, Yves. "Preliminary investigation of use of flexible folding wing tips for static and dynamic load alleviation". In: *The Aeronautical Journal* 121.1235 (2017), pp. 73–94.
- [14] Cheung, Ronald CM, Rezgui, Djamel, Cooper, Jonathan E, and Wilson, Thomas. "Testing of a hinged wingtip device for gust loads alleviation". In: *Journal of Aircraft* 55.5 (2018), pp. 2050–2067.
- [15] Cheung, Ronald CM, Rezgui, Djamel, Cooper, Jonathan E, and Wilson, Thomas. "Testing of folding wingtip for gust load alleviation of flexible high-aspect-ratio wing". In: *Journal of Aircraft* 57.5 (2020), pp. 876–888.
- [16] Healy, Fintan, Rezgui, Djamel, and Cooper, Jonathan E. "Experimental Effect of Sideslip Angle on the Dynamic Behaviour of Flared Folding Wingtips". In: *AIAA SCITECH 2023 Forum*. 2023, p. 0376.
- [17] Healy, Fintan J and Healy, Fintan J. "The Impact of Geometric Nonlinearities on the Behaviour of Floating Wingtips". In: *Aircraft Design* 82 (2023), pp. 1–23.
- [18] Healy, Fintan, Cheung, Ronald, Neofet, Theodor, Lowenberg, Mark, Rezgui, Djamel, Cooper, Jonathan, Castrichini, Andrea, and Wilson, Tom. "Folding wingtips for improved roll performance". In: *Journal of Aircraft* 59.1 (2022), pp. 15–28.
- [19] David, Christophe, Delbecq, Scott, Defoort, Sebastien, Schmollgruber, Peter, Benard, Emmanuel, and Pommier-Budinger, Valerie. "From FAST to FAST-OAD: An open source framework for rapid Overall Aircraft Design". In: *IOP Conference Series: Materials Science and Engineering*. Vol. 1024. https://doi.org/10.1088/1757-899X/1024/1/012062. IOP Publishing. 2021, p. 012062.
- [20] Benaouali, Abdelkader and Kachel, Stanisław. "Multidisciplinary design optimization of aircraft wing using commercial software integration". In: Aerospace Science and Technology 92 (2019), pp. 766–776.
- [21] Delbecq, Scott. "Knowledge-based multidisciplinary sizing and optimization of embedded mechatronic systems-application to aerospace electro-mechanical actuation systems". PhD thesis. Toulouse, INSA, 2018.
- [22] Jan, R. "Energy Harvesting on Flexible Uavs". PhD Thesis supervised by Moschetta, Jean-Marc and Condomines, Jean-Philippe Dynamique des fluides Toulouse, ISAE 2023. PhD thesis. ISAE-Supaero, 2023. URL: http://www.theses.fr/2023ESAE0046/document.
- [23] Drela, Mark. "ASWING 5.81 Technical Description Unsteady Extension". en. In: MIT (2008).
- [24] Drela, Mark. "ASWING 5.86 Technical Description Steady Formulation". en. In: *MIT* (2009), p. 57.

Evaluation of ASWING for overall aircraft design of unconventional configurations.

- [25] Jan, R. Experimental validation of ASWING. Part I: Aerodynamics. Tech. rep. ASW-1. ISAE-Supaero, 2023.
- [26] Jan, R. Experimental validation of ASWING. Part II: Propellers. Tech. rep. ASW-2. ISAE-Supaero, 2023
- [27] Jan, R. Experimental validation of ASWING. Part III: Structure. Tech. rep. ASW-3. ISAE-Supaero, 2023.
- [28] Jan, R. Experimental validation of ASWING. Part IV: Aeroelasticity. Tech. rep. ASW-4. ISAE-Supaero, 2023.
- [29] Wolkovitch, Julian. Low-Speed Wind Tunnel Test on Joined Wing and Monoplane Configurations. Volume 1. Analysis of Results. Tech. rep. Nasa contractor report N00014-79-C-0953 or ACA Report 82-1. NASA, 1982.
- [30] Smith, Stephen C and Stonum, Ronald K. Experimental aerodynamic characteristics of a joinedwing research aircraft configuration. NASA Technical Memorandum NASA-TM-101083. NASA, 1989.
- [31] Niles, Donald E. Column and Plate Compressive Strengths of Aircraft Structural Materials: Extruded 14S-T Aluminum Alloy. Tech. rep. Technical note 1027. NACA, 1946.
- [32] Peery, David J. Aircraft structures. Courier Corporation, 2011.
- [33] Drela, Mark. "TASOPT 2.00". In: Massachusetts Inst. Technol., Cambridge, MA, USA, Rep (2010).
- [34] Drela, Mark. "An Integrated Approach to the Design-Optimization of an N+ 3 Subsonic Transport". In: *AIAA 28th Applied Aerodynamics Conference*. 2010.
- [35] Drela, Mark. "Development of the D8 transport configuration". In: *29th AIAA Applied Aerody-namics Conference*. 2011, p. 3970.
- [36] Greitzer, Edward M, Bonnefoy, PA, DelaRosaBlanco, E, Dorbian, CS, Drela, M, Hall, DK, Hansman, RJ, Hileman, JI, Liebeck, RH, Lovegren, J, et al. *N+ 3 aircraft concept designs and trade studies*. Tech. rep. NASA, 2010.
- [37] Company, Boeing Commercial Airplane. 737 Airplane Characteristics for Airport Planning. Boeing Commercial Airplanes, 2005.
- [38] Company, Boeing Commercial Airplane. 777-200/-300 Airplane Characteristics for Airport Planning. Boeing Commercial Airplanes, 2022.
- [39] Company, Embraer. Embraer E195, Airport Planning Manuel. Embraer Company, 2022.